OFFICE OF NAVAL RESEARCH

Contract N7onr-35810

[illegible]

Technical Report No. [illegible]

[illegible]

[illegible]

[illegible]

GRADUATE DIVISION OF APPLIED MATHEMATICS

BROWN UNIVERSITY

PROVIDENCE, R. I.

January, 1954

[illegible]

PLASTIC DEFORMATIONS OF A FREE RING UNDER CONCENTRATED DYNAMIC LOADING[1]

by

Robert H. Owens[2] and P. S. Symonds[3]
(Brown University)

Summary

A concentrated time-dependent force acts on an unsupported thin ring along a diameter. The problem considered in this paper is to determine the deformations of the ring when the force magnitudes are such that plastic strains large compared with elastic strains occur. By neglecting elastic strains and assuming ideally plastic behavior, approximations to the final deformations of the ring are obtained. The analysis is developed for force pulses of arbitrary shape, but numerical results are obtained only in the special case of a rectangular force pulse. A criterion is stated for conditions when this type of analysis can be expected to provide satisfactory results.

1. Introduction

This analysis is an extension to an unsupported ring of ductile material of the methods employed in [1,3,4][4]. These references dealt with large plastic deformations of beams subjected to dynamic loading, under conditions such that elastic deformations could be disregarded.

The hypothesis that a satisfactory approximation to the final deformation in the ring subjected to a concentrated, dynamic load (Fig. 2) can be obtained by ignoring elastic strains (and hence elastic vibrations) leads to a "plastic-rigid" type of theory. Briefly, this theory assumes that the ring remains rigid until the moment developed in the ring.

---

1. The results in this paper were obtained in the course of research conducted under Contract N7onr-35810 between the Office of Naval Research and Brown University.

2. Research Associate in the Graduate Division of Applied Mathematics.

3. Associate Professor of Engineering.

4. Numbers in square brackets refer to the bibliography at the end of the paper.

at some section attains a value M_o, the yield or limit moment. At this section, unlimited bending may occur while the moment equals M_o. That is, the tangents on either side of this section may ultimately make a finite angle with one another. Such a material is described by Fig. 1. As discussed in [1], one way of computing M_o is by the formula

$$M_o = \sigma_y Z_p \qquad (1.1)$$

where σ_y is the yield stress and Z_p is the sum of the first moments of the upper and lower halves of the section area under consideration about its neutral axis. When a section of the ring sustains the moment M_o, a plastic hinge is said to exist there, and the unlimited bending that transpires corresponds to free rotation at the hinge under constant motion.

This theory should yield useful approximations if the total energy absorbed in plastic flow greatly exceeds the elastic energy that can be stored in the ring. A criterion expressing this state of affairs is developed subsequently.

It is assumed that the middle line of the ring has radius r which is large enough to permit the analysis to be carried out as if all the material were concentrated at the middle line. The mass per unit length of the middle line will be denoted by m and the time dependent load by P(t). The configuration to be studied appears in Fig. 2 in which small changes in geometry are neglected.

2. Motion Immediately After Impact

There is uniform translation of the ring immediately after the load is applied and this effect persists until the bending

moment due to inertia forces attains the value M_o at certain sections of the ring.

Let it be assumed that these plastic regions first occur at $\varphi = 0, \pi$. By symmetry, the shear force $V = 0$ at $\varphi = \pi$, and $V = P/2$ at $\varphi = 0$. The moment $M(\varphi)$ at any cross-section may now be obtained as indicated in Fig. 3. Here the acceleration $\underline{a}$ is given by

$$P = 2\pi rma \qquad (2.1)$$

and

$$M(\varphi) = N_o r(1 - \cos\varphi) + M_o - \frac{Pr}{2}\sin\varphi + \int_0^{\varphi} mar(r\sin\varphi - r\sin\theta)d\theta$$

$$2rN_o = \int_0^{\pi} mar^2 \sin\theta d\theta = 2mar^2.$$

These two equations with (2.1) give the result

$$M(\varphi) = M_o[1 - \frac{Pr}{2M_o}\sin\varphi + \frac{Pr}{2M_o}\frac{\varphi}{\pi}\sin\varphi]. \qquad (2.2)$$

If additional plastic regions occur, they will be located at stationary points of $M(\varphi)$. Setting $dM/d\varphi = 0$ gives

$$\sin\varphi = (\pi - \varphi)\cos\varphi. \qquad (2.3)$$

From the equation $d^2M/d\varphi^2 = Pr/2\pi\,[(\pi - \varphi)\sin\varphi + 2\cos\varphi]$ it is seen that $d^2M/d\varphi^2 < 0$ only for $\pi/2 << \varphi \leq \pi$, the corresponding solution of (2.3) being at $\varphi = \pi$. This solution is already employed. The solution of interest is

$$\varphi_o \approx 1.11 \approx 64^o \quad \text{or} \quad \sin\varphi_o = (\pi - \varphi_o)\cos\varphi_o \qquad (2.4)$$

where $d^2M/d\varphi^2 > 0$ implying $M(\varphi)$ has a minimum there. Let the

load P be increased until this minimum attains the value $-M_0$ so that (2.2) gives the result

$$\frac{Pr}{M_0} = \frac{2\pi}{(\pi - \varphi_0)\sin\varphi_0} \approx 6.88 \tag{2.5}$$

which is the collapse load parameter for the ring. When Pr/M_0 exceeds this value, the ring contains four plastic hinges at $\varphi = 0, \xi, \pi, 2\pi - \xi$ and may be treated as a kinematic mechanism since the segments between hinges are rigid according to the basic hypothesis. As in [1] it is assumed that $\xi = \xi(t)$; in special cases $\xi(t)$ may turn out to be constant.

3. Equations of Motion for the Deforming Ring

Since the points ξ, $2\pi - \xi$ correspond to stationary values of $M(\varphi)$, there is no shear at these hinges. Free body diagrams of the two segments joined at $\varphi = \xi$ are given in Figs. 4 and 5 along with the notation to be used in the equations of motion. The centers of mass and moments of inertia with respect to mass centers are given by the expressions

$$\left.\begin{aligned} \bar{r}_0 &= \frac{2r}{\xi}\sin\frac{\xi}{2} & \bar{r}_\pi &= \frac{2r}{\pi - \xi}\cos\frac{\xi}{2} \\ I_0 &= \frac{mr^3}{\xi}[\xi^2 - 2(1 - \cos\xi)] & I_\pi &= \frac{mr^3}{\pi-\xi}[(\pi - \xi)^2 - 2(1 + \cos\xi)] \end{aligned}\right\} \tag{3.0}$$

Equations expressing rate of change of angular momentum for each segment may be written with respect to transverse axes whose origins are at the centers of mass of the respective segments. However, the origin for the quantities y_0, y_π is fixed. Although the mass of each segment changes because of the motion of the hinge at $\varphi = \xi$, Newton's equations may be used in the form

"summation of forces equals product of mass and acceleration of center of mass", and "summation of torques about center of mass equals product of moment of inertia about center of mass and angular acceleration", since the rate of transfer of momentum from one segment to the other across the hinge due to the changing mass is zero and hence no impulsive forces are applied at the hinge point.

The analysis is based on the six equations of motion for the two segments hinged instantaneously at ξ, together with two equations which express continuity of velocity at the hinge point ξ. It is shown in Appendix I that continuity of velocity ensures continuity of displacement; the acceleration is discontinuous, in general, at a moving hinge. Thus, eight equations are available for the determination of eight unknowns $\dot{y}_o$, $\dot{y}_\pi$, ω_o, ω_π, ξ, N_o, N_π, N_ξ. The first four quantities are linear and angular velocities while the last three are axial forces; definitions are given by Figs. 4 and 5.

The equations of motion and continuity equations at the hinge are derived in Appendix I making use of Figs. 4 and 5. The six equations of motion can be reduced to three by eliminating N_o, N_π, N_ξ. These together with the two continuity equations form a system of five simultaneous equations of the form

$$a_{i1}\ddot{y}_o + a_{i2}\ddot{y}_\pi + a_{i3}r\dot{\omega}_o + a_{i4}r\dot{\omega}_\pi + a_{i5}(\xi,\dot{\xi},\ \omega_o,\ \omega_\pi) = 0 \quad (3.1\text{-}3.5)$$

The five equations (3.1-3.5) are obtained by giving i in turn the values 1,2,3,4, and 5.

The following notation will be used:

$$\frac{mr^3}{M_o}(\omega_\pi - \omega_o) \equiv \omega \tag{3.6}$$

$$\frac{Pr}{M_o} = \mu \tag{3.7}$$

Then the coefficients a_{ij} are as follows:

$a_{11} = (1 - \cos\xi)(\xi - \sin\xi)$, $a_{12} = 0$,
$a_{13} = (1 - \cos\xi)^2 - 2\sin\xi(\xi - \sin\xi)$, $a_{14} = 0$,
$a_{15} = 2\sin\xi - \frac{\mu}{2}(1 - \cos\xi)$, $a_{21} = 0$,
$a_{22} = (1 + \cos\xi)(\pi - \xi - \sin\xi)$, $a_{23} = 0$,
$a_{24} = (1 + \cos\xi)^2 - 2\sin\xi(\pi - \xi - \sin\xi)$, $a_{25} = -2\sin\xi$,

$a_{31} = \xi$, $a_{32} = \pi - \xi$, $a_{33} = 1 - \cos\xi$,
$a_{34} = 1 + \cos\xi$, $a_{35} = -\frac{\mu}{2}$, $a_{41} = 1$,
$a_{42} = -1$, $a_{43} = \sin\xi$, $a_{44} = -\sin\xi$,
$a_{45} = -\omega\dot{\xi}\cos\xi$, $a_{51} = 0$, $a_{52} = 0$,
$a_{53} = 1 - \cos\xi$, $a_{54} = 1 + \cos\xi$, $a_{55} = -\omega\dot{\xi}\sin\xi$.

In order to express the accelerations $\ddot{y}_o$, $\ddot{y}_\pi$, $\dot{\omega}_o$, $\dot{\omega}_\pi$ explicitly in terms of ξ and μ let the equations (3.1-5) be considered as a system of five <u>algebraic</u> linear equations in the four unknowns $\ddot{y}_o$, $\ddot{y}_\pi$, $r\dot{\omega}_o$, $r\dot{\omega}_\pi$. These algebraic equations will be compatible and have a solution only if the determinant of the system vanishes. This condition is

$$|a_{ij}| = 0 \tag{3.8}$$

where the elements in the i^{th} row and j^{th} column are given above. This determinant may be split into three determinants by breaking up the last column. The result is the equation

$$D_1(\xi) - \frac{\mu}{2}\,\bar{D}_1(\xi) - \omega\dot{\xi}\,D_2(\xi) = 0 \qquad (3.9)$$

where D_1, $\bar{D}_1$, D_2 may be reduced to third order determinants by Chio's method [2] in which form they were used in the numerical computations. These results are listed in Appendix II.

The quantity $\mu + 2\,D_2/\bar{D}_1\,\dot{\xi}\omega \equiv D_1/\bar{D}_1$, obtainable from (3.9), is plotted against ξ in Fig. 7.

The vanishing of (3.9) means that (3.1-5) has a unique algebraic solution in $\ddot{y}_o$, $\ddot{y}_\pi$, $r\dot{\omega}_o$, $r\dot{\omega}_\pi$ which may be obtained by eliminating the $\dot{\xi}$ terms from (3.4,5) and using the resulting equation with (3.1-3). This equation is

$$\sin\xi\ddot{y}_o - \sin\xi\ddot{y}_\pi + (1 - \cos\xi)r\dot{\omega}_o - (1 + \cos\xi)r\dot{\omega}_\pi = 0, \quad (3.10)$$

Cramer's rule will solve the algebraic system (3.1-3, 10). The denominator in Cramer's formula is

$$\Delta(\xi) = |b_{ij}| \qquad (3.11)$$

where the elements in the i^{th} row and j^{th} column are

$$b_{ij} = a_{ij} \quad \text{for} \quad i \leq 3, \quad j \leq 4,$$

and

$$b_{41} = -b_{42} = \sin\xi, \quad b_{43} = 1 - \cos\xi, \quad b_{44} = -(1 + \cos\xi).$$

Let $\Delta_i(\mu,\xi)$ denote the determinant obtained from $\Delta(\xi)$ by replacing the i^{th} column of $\Delta(\xi)$ by the negative of the "constant" terms of (3.1-3, 10), i.e., the terms not containing the algebraic unknowns. Then Cramer's rule states that

$$\ddot{y}_o = \frac{\Delta_1(\mu,\xi)}{\Delta(\xi)}, \quad \ddot{y}_\pi = \frac{\Delta_2(\mu,\xi)}{\Delta(\xi)}, \quad r\dot{\omega}_o = \frac{\Delta_3(\mu,\xi)}{\Delta(\xi)}, \quad r\dot{\omega}_\pi = \frac{\Delta_4(\mu,\xi)}{\Delta(\xi)}. \qquad (3.12)$$

In particular

$$r(\dot{\omega}_\pi - \dot{\omega}_0) = \frac{\Delta_4(\mu,\xi) - \Delta_3(\mu,\xi)}{\Delta(\xi)}$$

and since Δ_4 and Δ_3 differ in only one column, they may be combined, giving

$$\dot{\omega}\Delta(\xi) = |c_{ij}| \tag{3.13}$$

where the elements in the i^{th} row and j^{th} column are

$$c_{11} = (1 - \cos\xi)(\xi - \sin\xi),$$

$$c_{12} = (1 - \cos\xi)(\xi - \sin\xi),$$

$$c_{13} = (1 - \cos\xi)^2 - 2\sin\xi(\xi - \sin\xi),$$

$$c_{14} = -2\sin\xi + \frac{\mu}{2}(1 - \cos\xi),$$

$$c_{21} = 0,$$

$$c_{22} = (1 + \cos\xi)(\pi - \xi - \sin\xi),$$

$$c_{23} = (1 + \cos\xi)^2 - 2\sin\xi(\pi - \xi - \sin\xi),$$

$$c_{24} = 2\sin\xi,$$

$$c_{31} = \xi, \quad c_{32} = \pi, \quad c_{33} = 2, \quad c_{34} = \frac{\mu}{2},$$

$$c_{41} = \sin\xi, \quad c_{42} = 0, \quad c_{43} = -2\cos\xi, \quad c_{44} = 0.$$

If the last column of (3.13) is broken up so that two determinants are formed, equation (3.13) becomes

$$\dot{\omega}D_2(\xi) = D_3(\xi) - \frac{\mu}{2}\bar{D}_3(\xi) \tag{3.14}$$

where D_3, $\overline{D}_3$ may be reduced by Chio's method to third order determinants and are listed in Appendix II, and $D_2(\xi)$ can be shown to be identical with $\Delta(\xi)$.

The derivation of the equations expressing continuity across the hinge in Appendix I shows that

$$(1 - \cos \xi)\omega_0 + (1 + \cos \xi)\omega_\pi = 0. \tag{3.15}$$

Consequently, if ω is known ω_0 and ω_π follow from (3.6) and (3.15). Then the deformations, as shown in Appendix I may be obtained by integrating $d\Theta_0/dt = \omega_0$, $d\Theta_\pi/dt = \omega_\pi$ giving Θ_0, Θ_π as defined in Fig. 6. The problem, therefore, is to solve the pair of equations (3.9) and (3.14).

4. Solution for Rectangular Force Pulse

Numerical results for the special case of a rectangular force pulse are obtained.

Let $\dot{\xi} = 0$ so that ξ = const. It follows from (3.9) that $\mu/2 = D_1(\xi)/\overline{D}_1(\xi)$ = const. which is necessarily greater than 3.44, since all the equations under consideration are valid only when the hinge at $\varphi = \xi$ is present, i.e., when $\mu > 6.88$ by (2.5). The variation of ξ with μ may be obtained from Fig. 7 on putting $\dot{\xi} = 0$. Under the impact $\mu > 6.88$ the hinge moves instantaneously to the corresponding position given by Fig. 7. Let P = const. act for a time T after which $P \equiv 0$. Let ξ_0 be the corresponding hinge position, obtained from Fig. 7. Then $\dot{\omega}$ = const. which, from (3.14) gives

$$\omega = \frac{D_3(\xi_0) - \frac{\mu}{2}\overline{D}_3(\xi_0)}{D_2(\xi_0)} t, \quad 0 < t \leq T \tag{4.1}$$

where the constant of integration is zero since $\omega = 0$ for $t = 0$. Putting T for t gives the final value ω_T of ω under the load P.

$$\frac{\omega_T}{T} = \frac{D_3(\xi_o) - \frac{\mu}{2}\bar{D}_3(\xi_o)}{D_2(\ _o)} . \tag{4.2}$$

From (3.6) and (3.15)

$$\omega \equiv \frac{2}{1 - \cos\xi}\frac{mr^3}{M_o}\omega_\pi = -\frac{2}{1 + \cos\xi}\frac{mr^3}{M_o}\omega_o. \tag{4.3}$$

It can be seen from (4.3) that neglecting ω_o^2, ω_π^2 is equivalent to neglecting ω^2. Therefore, by (4.2), the restriction that T be sufficiently small and decrease as P increases must be enforced.

The equations $d\theta_o/dt = \omega_o$, $d\theta_\pi/dt = \omega_\pi$ combined with (4.3) give

$$\frac{mr^3}{M_o}\frac{d\theta_o}{dt} = -\frac{1}{2}(1 + \cos\xi_o)\omega, \tag{4.4}$$

$$\frac{mr^3}{M_o}\frac{d\theta_\pi}{dt} = \frac{1}{2}(1 - \cos\xi_o)\omega. \tag{4.5}$$

Introducing (4.1) into (4.4,5), performing the integration, and replacing t by T gives the final deformations θ_{oT}, $\theta_{\pi T}$ under the load.

$$\frac{mr^3}{M_o}\frac{\theta_{oT}}{T^2} = -\frac{1}{4}(1 + \cos\xi_o)\frac{\omega_T}{T} \tag{4.5a}$$

$$\frac{mr^3}{M_o}\frac{\theta_{\pi T}}{T^2} = \frac{1}{4}(1 - \cos\xi_o)\frac{\omega_T}{T}. \tag{4.5b}$$

When $T < t$, $P \equiv 0$ and (3.9, 14) reduces to

$$D_1(\xi) = \omega\dot{\xi}D_2(\xi) \tag{4.6}$$

$$\dot{\omega}D_2(\xi) = D_3(\xi) \quad \text{or} \quad D_3(\xi) = \frac{d\omega}{d\xi}\dot{\xi}D_2(\xi). \tag{4.7}$$

Dividing (4.7) by (4.6) gives the differential equation

$$\frac{d\omega}{\omega} = \frac{D_3(\xi)}{D_1(\xi)}\, d\xi, \tag{4.8}$$

which may be integrated, (4.2) serving as the initial condition, giving

$$\omega(\xi, \xi_o) = \omega_T \exp \int_{\xi_o}^{\xi} \frac{D_3(\xi)}{D_1(\xi)}\, d\xi \,. \tag{4.9}$$

Then, it follows from (4.6) that

$$\mathring{\xi} = \frac{D_1(\xi)}{D_2(\xi)} \frac{1}{\omega_T} \exp\left(- \int_{\xi_o}^{\xi} \frac{D_3(\xi)}{D_1(\xi)}\, d\xi\right) \tag{4.10}$$

Operating with the third order determinants in Appendix II and expanding each element in power series in $\pi/2 - \xi$ it can be shown that $D_1(\xi) = - a(\pi/2 - \xi) + \dots$, $D_2(\xi) = b + \dots$, $D_3(\xi) = c + \dots$, where a, b, c are positive numbers with $0 < c/a < 1/2$. Consequently, for ξ near $\pi/2$, ω/T behaves like $(\omega_T/T)(\pi/2 - \xi)^{c/a}$ and tends to zero as ξ tends to $\pi/2$. That is, the relative rotation of the two ring segments terminates when $\xi = \pi/2$ in view of (4.3). Therefore, final deformations Θ_{of}, $\Theta_{\pi f}$ may be obtained by integrating $d\Theta_o/dt = (d\Theta_o/d\xi)\dot{\xi}$, $d\Theta_\pi/dt = (d\Theta_\pi/d\xi)\dot{\xi}$ up to $\xi = \pi/2$. Using these latter relations with (4.4, 5) gives the results

$$\frac{mr^3}{M_o} \frac{\Theta_{of}}{T^2} = \frac{mr^3}{M_o} \frac{\Theta_{oT}}{T^2} - \frac{1}{2} \int_{\varphi}^{\pi/2} (1 + \cos \xi) \frac{\frac{\omega}{T}}{T\dot{\xi}}\, d\xi \tag{4.11}$$

$$\frac{mr^3}{M_o} \frac{\Theta_{\pi f}}{T^2} = \frac{mr^3}{M_o} \frac{\Theta_{\pi T}}{T^2} + \frac{1}{2} \int_{\varphi}^{\pi/2} (1 - \cos \xi) \frac{\frac{\omega}{T}}{T\dot{\xi}}\, d\xi, \tag{4.12}$$

where the first terms on the right of (4.11, 12) follow from (4.2) and (4.5a, 5b). Since $T\dot{\xi}$ behaves like $(\pi/2 - \xi)^{1-c/a}$ when ξ is near $\pi/2$, $T\dot{\xi} \to 0$ as $\xi \to \pi/2$. Moreover, $\omega/T/T\dot{\xi}$ behaves like $(\pi/2 - \xi)^{2c/a-1}$ so that the improper integrals in (4.11, 12) exist.

Numerical integration must be used on the above formulas. Since all the integrands have infinite singularities at $\pi/2$, numerical methods will be used up to $\xi = 1.5$ from which point the integrands are approximated to by the terms in their power series up to $(\pi/2 - \xi)$. For this reason the formulas (4.11, 12) will be modified. Put

$$\Phi(\xi,\varphi) = (1 + \cos\xi)\,\frac{\frac{\omega}{T}}{T\dot{\xi}} \tag{4.13}$$

$$\psi(\xi,\varphi) = (1 - \cos\xi)\,\frac{\frac{\omega}{T}}{T\dot{\xi}}\,. \tag{4.14}$$

From the expansions given above for D_1, D_2, D_3 it can be shown that for $1.5 \le \xi \le \pi/2$

$$\Phi(\xi,\varphi) \approx \left(1 + \frac{\pi}{2} - \xi\right)\left[\frac{\omega(1.5,\varphi)}{T}\right]^2 \frac{b}{a}\,\frac{(\pi/2 - \xi)^{2c/a-1}}{(\pi/2 - 1.5)^{2c/a}}, \quad 1.5 \le \xi \le \pi/2 \tag{4.15}$$

$$\psi(\xi,\varphi) \approx \left[1 - \left(\frac{\pi}{2} - \xi\right)\right]\left[\frac{\omega(1.5,\varphi)}{T}\right]^2 \frac{b}{a}\,\frac{(\pi/2 - \xi)^{2c/a-1}}{(\pi/2 - 1.5)^{2c/a}}, \quad 1.5 \le \xi \le \pi/2. \tag{4.16}$$

Then (4.11, 12) become

$$\frac{mr^3}{M_o}\frac{\Theta_{of}}{T^2} = \frac{mr^3}{M_o}\frac{\Theta_{oT}}{T^2} - \frac{1}{2}\int_{\varphi}^{1.5}\Phi(\xi,\varphi)\,d\xi - \frac{1}{2}\frac{b}{a}\left[\frac{\omega(1.5,\varphi)}{T}\right]^2\left(\frac{a}{2c} + \frac{\frac{\pi}{2} - 1.5}{\frac{2c}{a} + 1}\right) \tag{4.17}$$

$$\frac{mr^3}{M_o}\frac{\theta_{\pi f}}{T^2} = \frac{mr^3}{M_o}\frac{\theta_{\pi T}}{T^2} + $$
$$+ \frac{1}{2}\int_{\varphi}^{1.5}\psi(\xi,\varphi)d\xi + \frac{1}{2}\frac{b}{a}\left[\frac{\omega(1.5,\varphi)}{T}\right]^2\left(\frac{a}{2c} - \frac{\pi/2 - 1.5}{2c/a + 1}\right), \tag{4.18}$$

which are the expressions for deformations used in the computations. The resulting deformation parameters are plotted against μ in Fig. 8.

5. Check on Numerical Results

When relative rotation of the two ring segments ceases, the velocities $\dot{y}_o$, $\dot{y}_\pi$ must be equal as shown by (7.12). Then, either one may be used to compute momentum of the ring. The equation $\int_0^{t_f} Pdt = 2\pi rm\dot{y}_o = 2\pi rm\dot{y}_\pi$, where t_f is the time when the deformation terminates, leads to the formula

$$\mu = 2\pi\frac{mr^2}{M_o}\frac{\dot{y}_o}{T} = 2\pi\frac{mr^2}{M_o}\frac{\dot{y}_\pi}{T} \tag{5.1}$$

since $\int_0^{t_f} Pdt = PT$. From (3.12) and the remark following (3.14) concerning $D_2(\xi)$ it follows that

$$\frac{mr^2}{M_o}\ddot{y}_o = \frac{D_o(\xi) - \frac{\mu}{2}\bar{D}_o(\xi)}{D_2(\xi)} \tag{5.2}$$

$$\frac{mr^2}{M_o}\ddot{y}_\pi = \frac{D_\pi(\xi) - \frac{\mu}{2}\bar{D}_\pi(\xi)}{D_2(\xi)} \tag{5.3}$$

where D_o, $\bar{D}_o$ are derivable from $\Delta_1(\mu,\xi)$; D_π, $\bar{D}_\pi$ from $\Delta_2(\mu,\xi)$ of (3.12). These determinants, after reduction to 3rd order, are

listed in Appendix II. Integration is performed while μ is constant, the results at $t = T$ being

$$\frac{mr^2}{M_o}\frac{\dot{y}_{oT}}{T} = \frac{D_o(\varphi) - \frac{\mu}{2}\bar{D}_o(\varphi)}{D_2(\varphi)} \tag{5.4}$$

$$\frac{mr^2}{M_o}\frac{\dot{y}_{\pi T}}{T} = \frac{D_\pi(\varphi) - \frac{\mu}{2}\bar{D}_\pi(\varphi)}{D_2(\varphi)} . \tag{5.5}$$

For $T < t$, $\mu = 0$ and equations (5.2, 3) become

$$\frac{mr^2}{TM_o}\frac{d\dot{y}_o}{d\xi} = \frac{D_o(\xi)}{T\dot{\xi}D_2(\xi)} \equiv - A(\xi,\varphi) \tag{5.6}$$

$$\frac{mr^2}{TM_o}\frac{d\dot{y}_\pi}{d\xi} = \frac{D_\pi(\xi)}{T\dot{\xi}D_2(\xi)} \equiv B(\xi,\varphi). \tag{5.7}$$

Approximations for A and B when $1.5 \leq \xi \leq \pi/2$ are obtained in the same manner as before with $D_o = c/2 + 2\pi(\pi/2 - \xi) + \ldots$, $D_\pi = - c/2 + 2\pi(\pi/2 - \xi) + \ldots$. Then

$$A(\xi,\varphi) = \frac{\omega(1.5,\varphi)}{Ta(\frac{\pi}{2} - 1.5)^{c/a}}\left\{\frac{c}{2}(\frac{\pi}{2} - \varphi)^{c/a-1} + 2\pi(\frac{\pi}{2} - \varphi)^{c/a}\right\}, \quad 1.5 \leq \xi \leq \pi/2 \tag{5.8}$$

$$B(\xi,\varphi) = \frac{\omega(1.5,\varphi)}{Ta(\frac{\pi}{2} - 1.5)^{c/a}}\left\{\frac{c}{2}(\frac{\pi}{2} - \varphi)^{c/a-1} - 2\pi(\frac{\pi}{2} - \varphi)^{c/a}\right\}, \quad 1.5 \leq \xi \leq \pi/2. \tag{5.9}$$

Using these approximations, integration of (5.6, 7) up to $\xi = \pi/2$ gives

$$\frac{mr^2}{M_o}\frac{\dot{y}_o}{T} = \frac{mr^2}{M_o}\frac{\dot{y}_{oT}}{T} - \int_\varphi^{1.5} A(\xi,\varphi)d\xi - \frac{\omega(1.5,\varphi)}{T}\left[\frac{1}{2} + \frac{2\pi}{a+c}(\frac{\pi}{2} - 1.5)\right] \tag{5.10}$$

$$\frac{mr^2}{M_o}\frac{\dot{y}_\pi}{T} = \frac{mr^2}{M_o}\frac{\dot{y}_{\pi T}}{T} + \int_\varphi^{1.5} B(\xi,\varphi)d\xi + \frac{\omega(1.5,\varphi)}{T}\left[\frac{1}{2} - \frac{2\pi}{a+c}(\frac{\pi}{2} - 1.5)\right] \tag{5.11}$$

Equations (5.10, 11) may be introduced into (5.1) as a check on the numerical work performed. In particular, the graph of the right members of (5.1) versus φ should coincide with Fig. 7 since this figure is essentially μ versus ξ. The error shown there is smallest for $\dot{y}_\pi$, as expected, because (5.11) involves addition only of small numbers. The error in $\dot{y}_0$ is much larger since the subtraction indicated by (5.10) involves two large numbers. Error in $\dot{y}_\pi$ ranges from 9% for large μ to practically zero for small μ.

As discussed in [1] an analysis of plastic deformations in which strains of elastic magnitude are neglected can be expected to give satisfactory results when the energy absorbed in plastic deformation greatly exceeds the maximum <u>elastic</u> strain energy that could be stored in the ring. This furnishes a means of estimating the range of validity of this type of analysis. The maximum elastic strain energy can be estimated as

$$W_\epsilon = \int_0^{2\pi} \frac{M_o^2 \cos^2\varphi \; r d\varphi}{2EI} = \frac{\pi}{2} \frac{M_o^2}{EI}.$$

The work of plastic deformation is given approximately by

$$W_p = 2M_o\Theta_{of}.$$

Hence the requirement for validity of the assumption that elastic deformations are negligible is

$$2M_o\Theta_{of} >> \frac{\pi}{2} \frac{M_o^2 r}{EI} . \qquad (5.12)$$

The dimensionless deformation parameter $mr^3\Theta_{of}/M_oT^2$ is a function

of μ_o only, as plotted in Fig. 8. The inequality criterion can be rewritten as

$$\frac{mr^3\theta_{of}}{M_o T^2} = f(\mu_o) >> \frac{\pi}{4} \frac{mr^4}{EIT^2} . \qquad (5.13)$$

The period τ of the lowest flexural mode of free vibration of the ring is given by

$$\tau = 2\pi \frac{\sqrt{5}}{6} \sqrt{\frac{mr^4}{EI}} .$$

Hence the inequality above can be expressed as

$$\frac{mr^3\theta_{of}}{M_o T^2} = f(\mu_o) >> \frac{9}{20\pi} \frac{\tau^2}{T^2} = 0.14 \frac{\tau^2}{T^2} . \qquad (5.14)$$

This inequality, in conjunction with Fig. 8, provides a convenient means of estimating the value of the load μ_o, for a given period ratio τ/T, above which the neglect of elastic deformations in the present analysis can be expected to be justified. Conversely, for a given load magnitude μ_o the above inequality can be used to estimate the upper limit of the ratio τ/T above which the present results should be valid.

The present results for a rectangular force pulse can probably be used to obtain fair estimates of the deformations which force pulses of quite different shapes will produce. Solutions of other problems [3], [4] have been carried out for a variety of force pulse shapes, e.g., a half-sine pulse, a triangular, or an exponential pulse, as well as for a rectangular pulse. Comparison of the results of these solutions shows that the curves of dimensionless deformation (analogous to that plotted in Fig. 8) for the rectangular pulse of duration T, and maximum

dimensionless load μ_o give reasonably good values of the same dimensionless parameter for other force pulse shapes, provided in all cases μ_o stands for the peak load and T stands for the time such that $\mu_o T$ is the total impulse $\int_0^\infty \mu dt$. Hence the dimensionless deformations plotted in Fig. 7 can be used tentatively to estimate the corresponding quantity for force pulses of general shape, by interpreting μ_o as the peak (dimensionless) load and T as the total impulse divided by peak load.

It should also be re-emphasized that the present analysis assumes that geometry changes can be neglected in the equations of motion, so that the results cannot be expected to hold when the distortions are very large. It would be desirable to investigate these and other neglected effects experimentally as well as analytically.

Bibliography

1. E. H. Lee and P. S. Symonds, "Large Plastic Deformation of Beams under Transverse Impact", Journal of Applied Mechanics, Trans. ASME, vol. 19, no. 3, 1952, pp. 308-314.

2. E. T. Whittaker and G. Robinson, "The Calculus of Observations", Blackie & Son, Limited, London, 4th Ed., p. 71.

3. P. S. Symonds, "Dynamic Load Characteristics in Plastic Bending of Beams", Journal of Applied Mechanics, vol. 20, no. 4, December, 1953.

4. P. S. Symonds, "Large Plastic Deformations of Beams under Blast Type Loading", Technical Report All-99 of Brown University to Office of Naval Research; paper presented at the Fourth Symposium on Plasticity, Brown University, Sept. 1-3, 1953.

Appendix I

6. The equations of motion for the lower segment may be obtained from Fig. 4. These are

$$\frac{P}{2} - N_\xi \sin \xi = mr\xi(\ddot{y}_o + \bar{r}_o \sin \frac{\xi}{2}\, \dot{\omega}_o) \tag{6.1}$$

$$N_o - N_\xi \cos \xi = - mr\xi(r - \bar{r}_o \cos \frac{\xi}{2})\dot{\omega}_o \tag{6.2}$$

$$2M_o + N_o(r - \bar{r}_o \cos \frac{\xi}{2}) - N_\xi(r - \bar{r}_o \cos \frac{\xi}{2}) - P \frac{\bar{r}_o}{2} \sin \frac{\xi}{2} = I_o\dot{\omega}_o. \tag{6.3}$$

After introducing into (6.1,2,3) the values for $\bar{r}_o$, I_o from equations (3.0) it follows from (6.1,2) that

$$N_o \sin \xi = \frac{P}{2} \cos \xi - mr\xi \cos \xi\ddot{y}_o + mr^2(1 - \cos \xi - \xi \sin \xi)\dot{\omega}_o \tag{6.4}$$

and from (6.1) that

$$N_\xi \sin \xi = \frac{P}{2} - mr\xi\ddot{y}_o - mr^2(1 - \cos \xi)\dot{\omega}_o. \tag{6.5}$$

Equation (3.1) results from combining (6.3,4,5).

Similarly the equations for the upper segment are obtained from Fig. 5.

$$N_\xi \sin \xi = mr(\pi - \xi)[\ddot{y}_\pi + \bar{r}_\pi \sin \frac{\pi - \xi}{2}\, \dot{\omega}_\pi] \tag{6.6}$$

$$N_\xi \cos \xi - N_\pi = mr(\pi - \xi)(r - \bar{r}_\pi \cos \frac{\pi - \xi}{2})\dot{\omega}_\pi \tag{6.7}$$

$$-2M_o + N_\pi(r - \bar{r}_\pi \cos \frac{\pi - \xi}{2}) + N_\xi(r - \bar{r}_\pi \cos \frac{\pi - \xi}{2}) = I_\pi\dot{\omega}_\pi. \tag{6.8}$$

Combining (6.6, 7), after introducing $\bar{r}_\pi$, I_π, from (3.0) gives

$$N_\pi \sin \xi = mr(\pi - \xi)\cos \xi\ddot{y}_\pi + mr^2[1 + \cos \xi - (\pi - \xi)\sin \xi]\dot{\omega}_\pi \tag{6.9}$$

and substituting this equation and (6.6) into (6.8) gives equation (3.2).

7. The Equations for displacement, velocity and acceleration at the moving hinge may be obtained in the following manner.

Let $\Theta \equiv \Theta(\varphi,t)$ denote the small angle through which each element $rd\varphi$ of the ring has rotated. Deformation due to tensile stresses will be neglected so that this rotation represents the deformation of each ring element. It follows from Fig. 9 that

$$dy = rd\varphi \sin(\Theta + \varphi) \approx r\Theta \cos \varphi d\varphi + r \sin \varphi d\varphi \tag{7.1}$$

$$dx = rd\varphi \cos(\Theta + \varphi) \approx r \cos \varphi d\varphi - r\Theta \sin \varphi d\varphi. \tag{7.2}$$

The existence of the plastic hinge at $\varphi = \xi$ implies different angular velocities for the two ring segments joined at the hinge. In general, then, the deformation function $\Theta(\varphi,t)$ will be different for the two ring segments. Let $\Theta_o = \Theta(\varphi,t)$, $\varphi < \xi$ and $\Theta_\pi = \Theta(\varphi,t)$, $\xi < \varphi$ so that $\partial\Theta_o/\partial t = \omega_o(t)$, $\partial\Theta_\pi/\partial t = \omega_\pi(t)$. Note that Θ_o and Θ_π may depend on φ, but ω_o, ω_π which describe the rigid motion of the lower and upper segments respectively of the ring, must depend on t alone. That these ring segments are rigid follows from the rigid-plastic hypothesis. For, the moment $M(\varphi)$ in the portion of the ring over which the hinge at ξ has passed is less than the limit moment M_o. The alternative is that $M(\varphi) = M_o$ and then $V = dM/rd\varphi = 0$. But $V \neq 0$ because of the presence of d'Alembert forces proporational to the local acceleration.

The deformation (relative rotation of the ring segments) generated at the moving hinge appears in the form of an increase in curvature since the hinge remains at no point for a finite time. This increase in curvature is given by

$$\frac{\frac{\partial\Theta_\pi}{\partial t} dt - \frac{\partial\Theta_o}{\partial t} dt}{r\dot{\xi}dt} = \frac{\omega_\pi - \omega_o}{r\dot{\xi}}. \tag{7.3}$$

Moreover, as long as the hinge moves no "kinks" appear so that

$$\Theta_o(\xi^-,t) = \Theta_\pi(\xi^+,t). \tag{7.4}$$

It follows from (7.1) that

$$y = y_o + r\int_0^\varphi \Theta_o \cos\varphi d\varphi + r\int_0^\varphi \sin\varphi d\varphi, \quad \varphi < \xi. \tag{7.5}$$

Differentiation with respect to time is denoted by dots. From (7.5)

$$\dot{y} = \dot{y}_o + r\omega_o\int_0^\varphi \cos\varphi d\varphi, \; \varphi < \xi \tag{7.6}$$

$$\ddot{y} = \ddot{y}_o + r\dot{\omega}_o\int_0^\varphi \cos\varphi d\varphi, \; \varphi < \xi. \tag{7.7}$$

<u>Remark</u>: The approximation made in (7.1, 2) is equivalent to neglecting ω_o^2, a restriction mentioned previously under (4.3), for if (7.7) were obtained without making this approximation, an additional term containing the factor ω_o^2 would appear.

When $\xi < \varphi$, it again follows from (7.1) that

$$y = y_o + r\int_0^\xi \Theta_o \cos\varphi d\varphi + r\int_\xi^\varphi \Theta_\pi \cos\varphi d\varphi + r\int_0^\varphi \sin\varphi d\varphi, \; \xi<\varphi \tag{7.8}$$

$$\dot{y} = \dot{y}_o + r\Theta_o(\xi^-,t)\dot{\xi}\cos\xi - r\Theta_\pi(\xi^+,t)\dot{\xi}\cos\xi + r\omega_o\int_0^\xi \cos\varphi d\varphi$$

$$+ r\omega_\pi\int_\xi^\varphi \cos\varphi d\varphi, \; \xi < \varphi. \tag{7.9}$$

This last equation simplifies on using (7.4) or, if the hinge

velocity is zero, deleting the terms containing $\dot{\xi}$ so that

$$\dot{y} = \dot{y}_0 + r\omega_0 \int_0^{\xi} \cos\varphi d\varphi + r\omega_\pi \int_{\xi}^{\varphi} \cos\varphi d\varphi, \quad \xi < \varphi \tag{7.10}$$

$$\ddot{y} = \ddot{y}_0 + r\dot{\omega}_0 \int_0^{\xi} \cos\varphi d\varphi + r\dot{\omega}_\pi \int_{\xi}^{\varphi} \cos\varphi d\varphi + r\cos\xi(\omega_0 - \omega_\pi)\dot{\xi}, \quad \xi < \varphi. \tag{7.11}$$

Now let $\varphi \longrightarrow \xi^-$ in (7.5, 6, 7) and $\varphi \longrightarrow \xi^+$ in (7.8, 10, 11). The results are that $y^- = y^+$, $\dot{y}^- = \dot{y}^+$, but $\ddot{y}^+ - \ddot{y}^- = r\cos\xi(\omega_0 - \omega_\pi)\dot{\xi}$. That is, vertical components of displacements and velocities are equal at the hinge, but accelerations are discontinuous, and they jump by the amount $r\cos\xi(\omega_0 - \omega_\pi)\dot{\xi}$.

Putting $\varphi = \pi$, $y = y_\pi$ in (7.10, 11) yields

$$\dot{y}_\pi = \dot{y}_0 + r\omega_0 \sin\xi - r\omega_\pi \sin\xi \tag{7.12}$$

$$\ddot{y}_0 - \ddot{y}_\pi + r\dot{\omega}_0 \sin\xi - r\dot{\omega}_\pi \sin\xi - r\cos\xi(\omega_\pi - \omega_0)\dot{\xi} = 0. \tag{7.13}$$

A similar analysis applies to the horizontal components. From (7.2)

$$x = r\int_0^{\varphi} \cos\varphi d\varphi - r\int_0^{\varphi} \Theta_0 \sin\varphi d\varphi, \quad \varphi < \xi \tag{7.14}$$

$$x = r\int_0^{\varphi} \cos\varphi d\varphi - r\int_0^{\xi} \Theta_0 \sin\varphi d\varphi - r\int_{\xi}^{\varphi} \Theta_\pi \sin\varphi d\varphi, \quad \xi < \varphi. \tag{7.15}$$

Differentiating these last two expressions yields the results that horizontal components of displacement and velocity are continuous across the hinge but acceleration jumps by the amount $r\sin\xi(\omega_\pi - \omega_0)\dot{\xi}$

Putting $\varphi = \pi$, $x = x_\pi \equiv 0$ into the differentiated forms

of (7.14, 15) gives

$$(1 - \cos \xi) r\omega_0 + (1 + \cos \xi) r\omega_\pi = 0 \qquad (7.16)$$

$$(1 - \cos \xi) r\dot{\omega}_0 + (1 + \cos \xi) r\dot{\omega}_\pi - \sin \xi r(\omega_\pi - \omega_0)\dot{\xi} = 0. \qquad (7.17)$$

Remark: (i) Equations (7.12, 16) may be obtained by requiring velocities to be equal at the hinge and (7.13, 17) may then be obtained by differentiation.

(ii) The quantities Θ_0, Θ_π defined by $\omega_0 = \partial\Theta_0/\partial t$, $\omega_\pi = d\Theta_\pi/\partial t$ are required. These deformations will be obtained only at $\varphi = 0$, as shown in Fig. 6. Since the hinge at ξ never reaches $\varphi = 0, \pi$, the desired deformation may be calculated from $d\Theta_0/dt = \omega_0$, $d\Theta_\pi/dt = \omega_\pi$ because of the rigid property of the ring in the vicinity of these points.

Appendix II

8. Below are forms of the various determinants as used in the computations where the elements in the i^{th} row and j^{th} column are denoted by a_{ij}.

$$D_o(\xi) = 2 \sin\xi(1 + \cos\xi)|d_{ij}| \tag{8.1}$$

where

$d_{11} = - d_{21} = 1$, $d_{12} = \sin\xi(1-\cos\xi) - 2(1+\cos\xi)(\xi-\sin\xi)$

$d_{13} = (1 - \cos\xi)^2 - 2\sin\xi(\xi - \sin\xi)$,

$d_{22} = (1 + \cos\xi)(\pi - \xi - \sin\xi)$

$d_{23} = - \frac{\sin\xi}{1+\cos\xi}[2(1-\cos\xi)(\pi-\xi-\sin\xi) - \sin\xi(1+\cos\xi)]$

$d_{31} = 0$, $d_{32} = \pi - \xi + \sin\xi$, $d_{33} = 2(1 - \cos\xi)$

$$\bar{D}_o(\xi) = (1 + \cos\xi)|e_{ij}| \tag{8.2}$$

where

$e_{11} = 1 - \cos\xi$, $e_{21} = 0$, $e_{31} = 1$, $e_{ij} = d_{ij}$ for $j = 2,3$.

$$D_\pi(\xi) = 2(1 + \cos\xi)\sin\xi|f_{ij}| \tag{8.3}$$

where

$f_{11} = - f_{21} = 1$, $f_{12} = - (1 - \cos\xi)(\xi - \sin\xi)$, $f_{13} = d_{13}$,

$f_{22} = - \sin\xi(1 + \cos\xi) + 2(1 - \cos\xi)(\pi - \xi - \sin\xi)$, $f_{23} = d_{23}$,

$f_{31} = 0$, $f_{32} = - (\xi + \sin\xi)$, $f_{33} = 2(1 - \cos\xi)$

$$\bar{D}_\pi(\xi) = (1 + \cos\xi)|g_{ij}| \tag{8.4}$$

where

$$g_{11} = 1 - \cos \xi, \quad g_{21} = 0, \quad g_{31} = 1, \quad g_{ij} = f_{ij} \text{ for } j = 2,3$$

$$D_1(\xi) = 2(1 + \cos \xi)|h_{ij}| \tag{8.5}$$

where

$$h_{11} = (1 - \cos \xi)(\xi - \sin \xi), \quad h_{12} = \sin \xi(1 - \cos \xi) - 4(\xi - \sin \xi)$$

$$h_{13} = - h_{23} = 1, \quad h_{21} = (1 + \cos \xi)(\pi - \xi - \sin \xi)$$

$$h_{22} = 2(1 - \cos \xi)(\pi - \xi - \sin \xi) - \sin \xi(1 + \cos \xi),$$

$$h_{31} = \pi(1 - \cos \xi), \quad h_{32} = - 2\xi(1 - \cos \xi), \quad h_{33} = 0$$

$$\overline{D}_1(\xi) = \sin \xi |k_{ij}| \tag{8.6}$$

where

$$k_{ij} = h_{ij} \quad \text{for} \quad j = 1,2 \quad \text{and } k_{13} = k_{33} = 1, \quad k_{23} = 0$$

$$D_2(\xi) = \sin \xi |\ell_{ij}| \tag{8.7}$$

where

$$\ell_{ij} = h_{ij} \quad \text{for} \quad j = 1,2 \quad \text{and} \quad \ell_{13} = \frac{4(\xi - \sin \xi)}{1 - \cos \xi} - \xi$$

$$\ell_{23} = 0, \quad \ell_{33} = \xi - \sin \xi$$

$$D_3(\xi) = 2 \sin \xi |m_{ij}| \tag{8.8}$$

where

$$m_{11} = h_{11}, \quad m_{12} = \sin \xi(1 - \cos \xi) - 2(\xi - \sin \xi), \quad m_{13} = - m_{23} = 1$$

$$m_{21} = h_{21}, \quad m_{22} = - \frac{1+\cos \xi}{1-\cos \xi}[2(1-\cos \xi)(\pi-\xi-\sin \xi)-\sin\xi(1+\cos\xi)]$$

$$m_{31} = h_{31}, \quad m_{32} = 2(\sin \xi + \xi \cos \xi), \quad m_{33} = 0$$

$$\overline{D}_3(\xi) = (1 - \cos \xi)|n_{ij}| \tag{8.9}$$

where

$$n_{ij} = m_{ij} \quad \text{for} \quad j = 1,2 \quad \text{and} \quad m_{13} = m_{33} = 1, \quad m_{23} = 0.$$

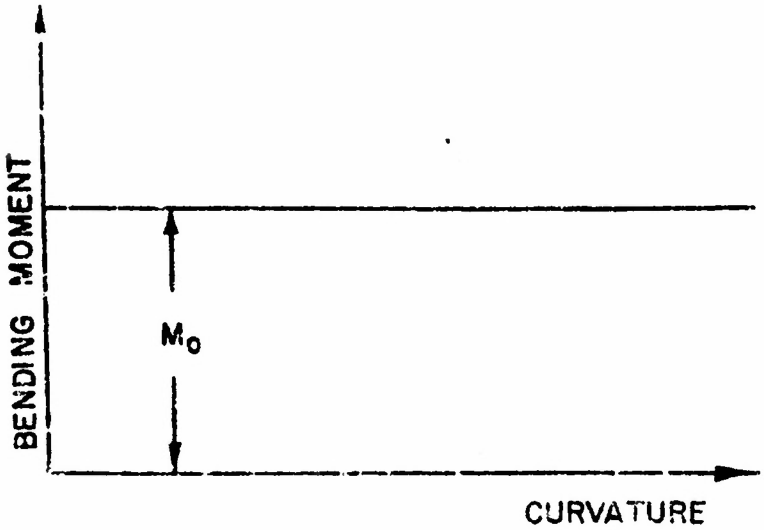

FIG. 1

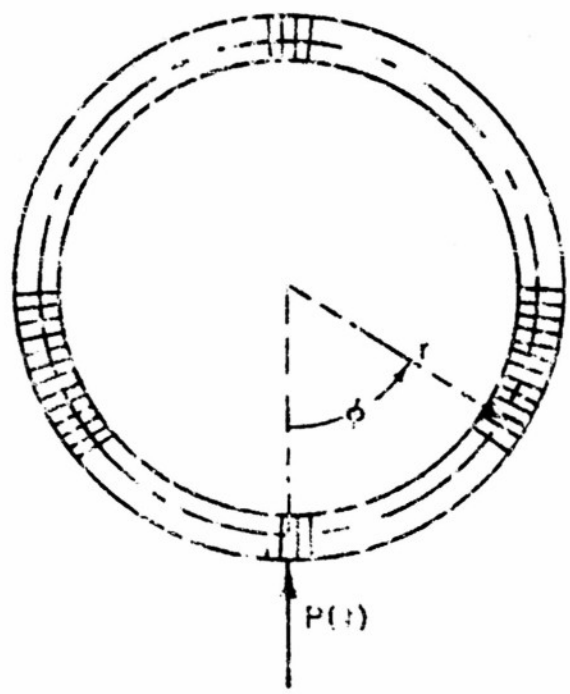

FIG. 2

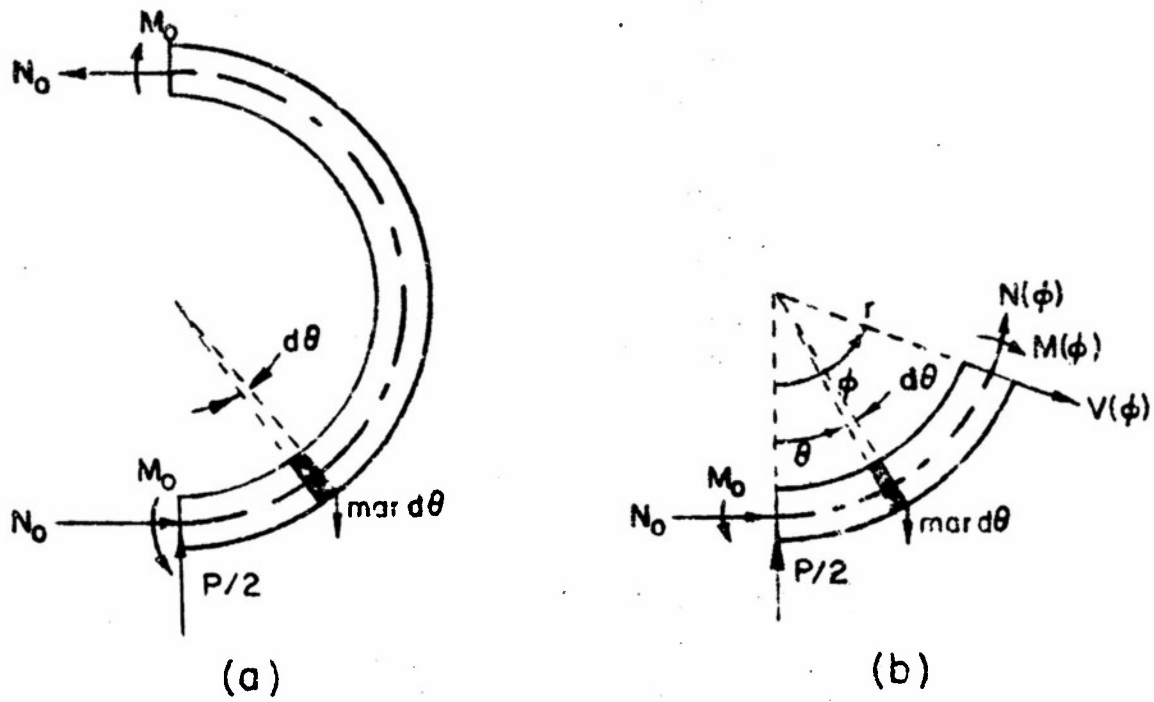

M_o
N_o
$d\theta$
M_o
N_o
$mar\,d\theta$
$P/2$
(a)
$N(\phi)$
$M(\phi)$
r
ϕ
$d\theta$
$V(\phi)$
θ
M_o
N_o
$mar\,d\theta$
$P/2$
(b)

FIG. 3

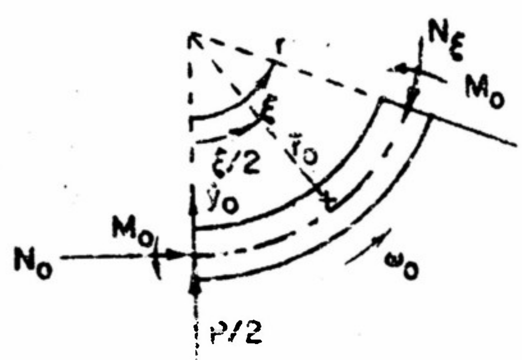

N_ξ
r
M_o
ξ
$\xi/2$
$\bar{y}_o$
$\dot{y}_o$
M_o
N_o
ω_o
$P/2$

FIG. 4

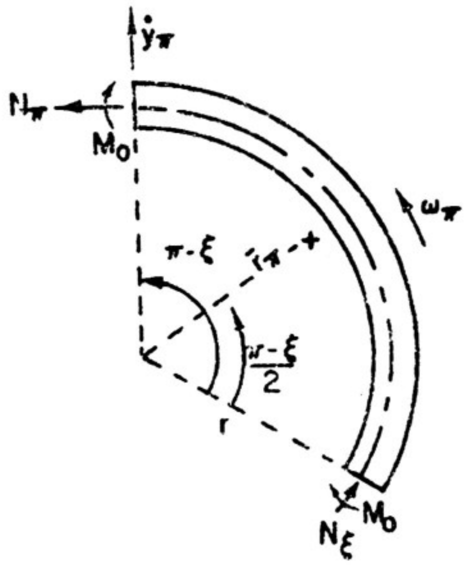
$\dot{y}_\pi$
N_π
M_0
ω_π
$\pi - \xi$
$\frac{\pi - \xi}{2}$
r
N_ξ
M_0

FIG. 5

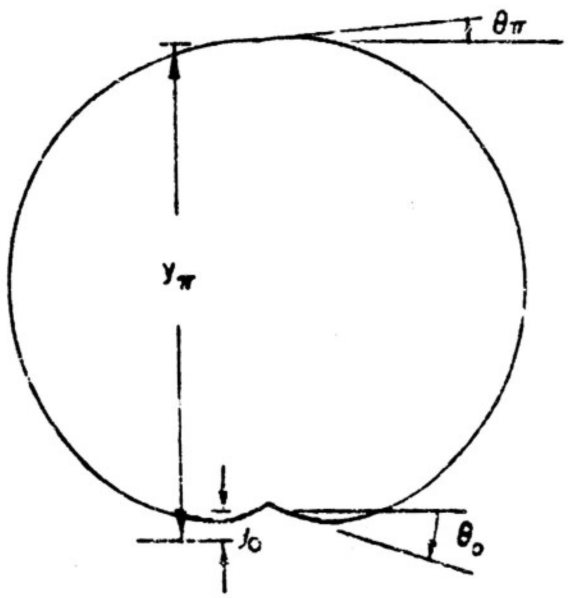
θ_π
y_π
y_0
θ_0

FIG. 6

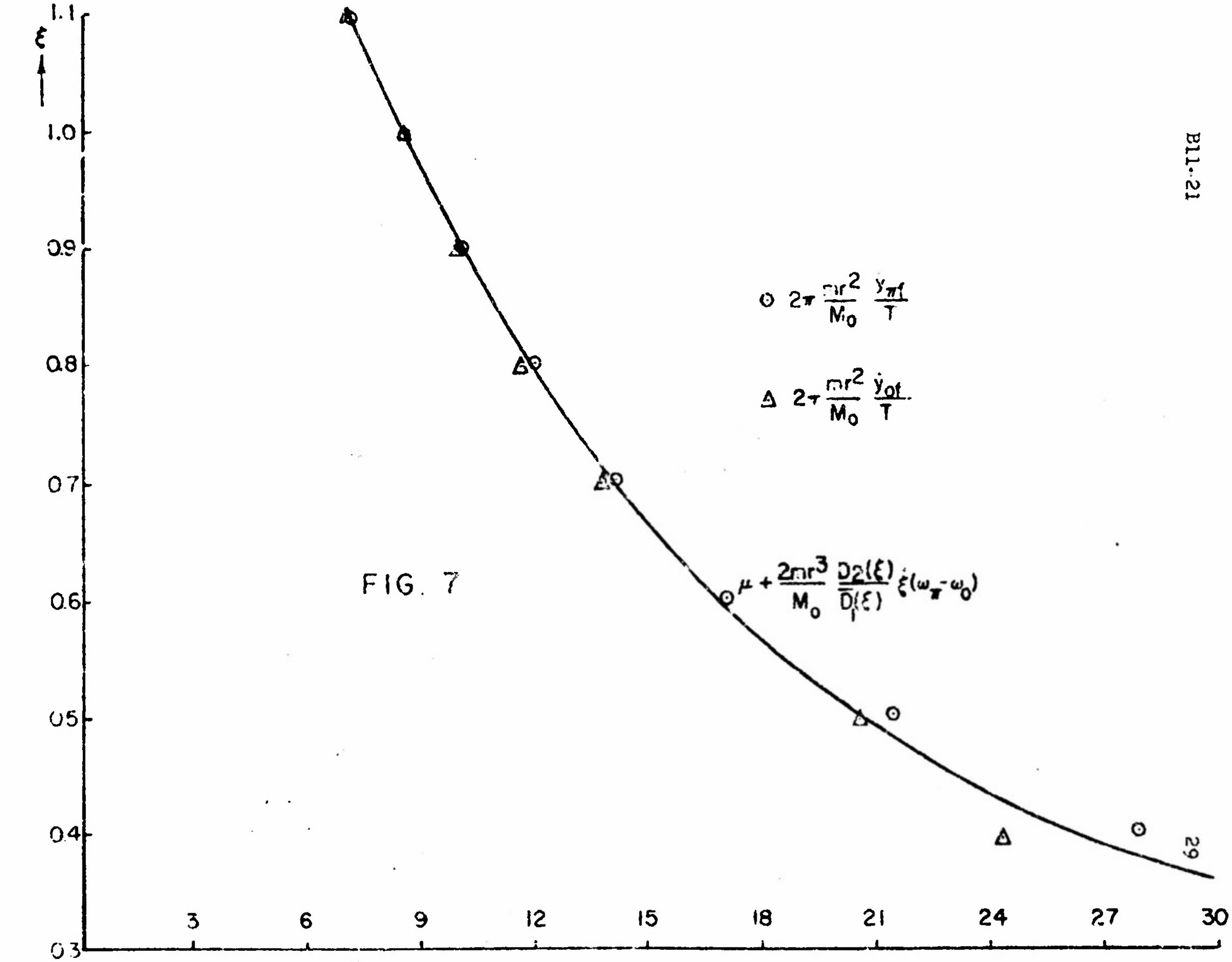

ξ
1.1
1.0
0.9
0.8
0.7
0.6
0.5
0.4
0.3
3
6
9
12
15
18
21
24
27
30
$\odot\ 2\pi \frac{mr^2}{M_0} \frac{y_{\pi f}}{T}$
$\Delta\ 2\pi \frac{mr^2}{M_0} \frac{\dot{y}_{0f}}{T}$
$\mu + \frac{2mr^3}{M_0} \frac{D_2(\xi)}{D_1(\xi)} \dot{\xi}(\omega_\pi - \omega_0)$

FIG. 7

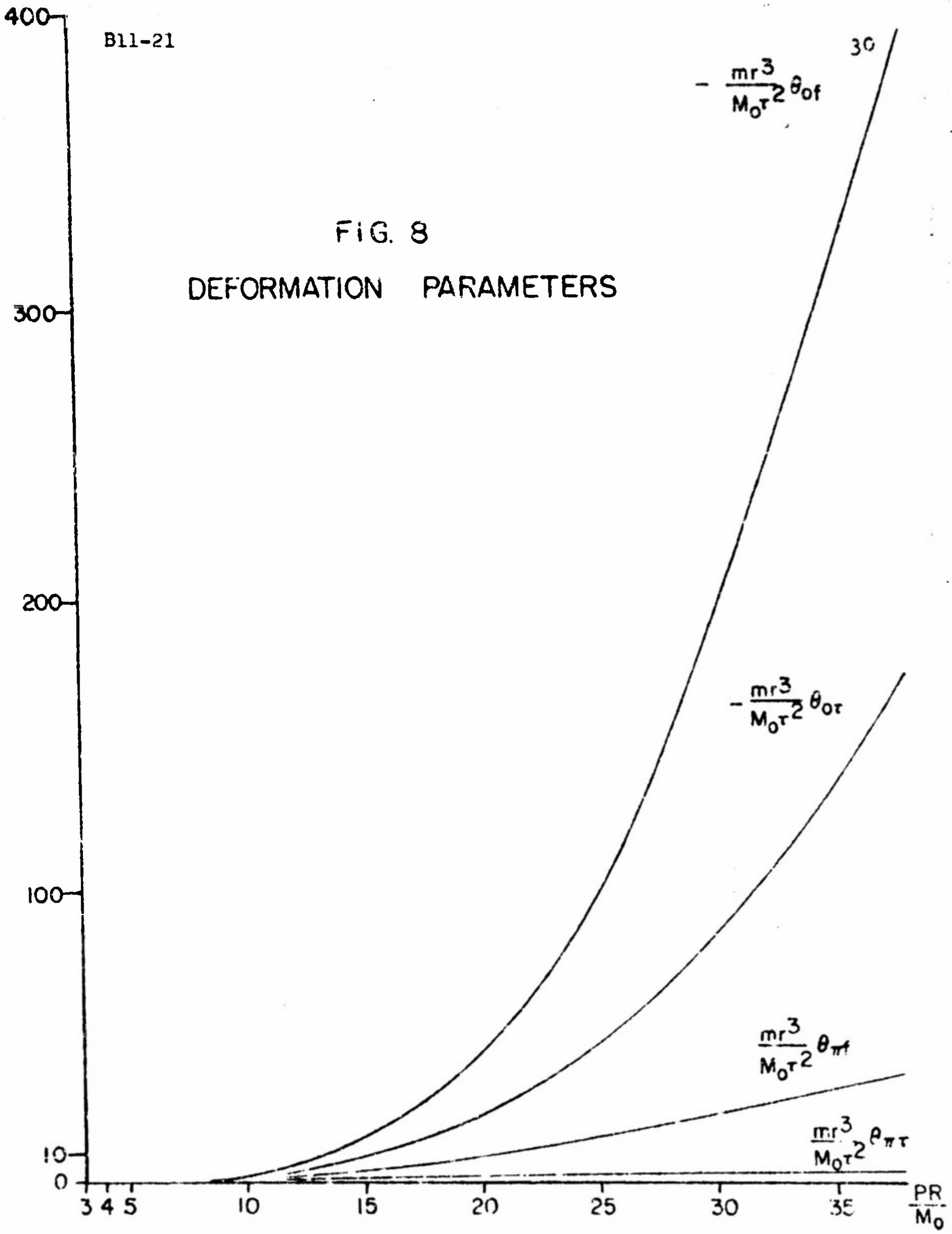

FIG. 8

DEFORMATION PARAMETERS

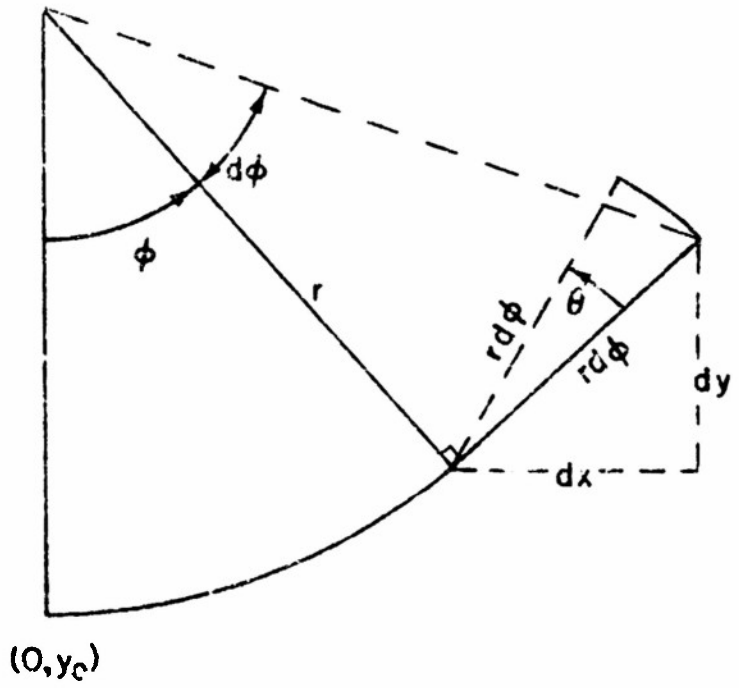

FIG. 9

Distribution List
for
Technical and Final Reports Issued Under
Office of Naval Research Project NR-360-364, Contract N7onr-35810

I: Administrative, Reference and Liaison Activities of ONR

Chief of Naval Research
Department of the Navy
Washington 25, D. C.
Attn: Code 438 (2)
Code 432 (1)
Code 466 (via Code 108) (1)

Director, Naval Research Lab.
Washington 25, D. C.
Attn: Tech. Info. Officer (9)
Technical Library (1)
Mechancics Division (2)

Commanding Officer
Office of Naval Research
Branch Office
495 Summer Street
Boston 10, Mass. (2)

Commanding Officer
Office of Naval Research
Branch Office
346 Broadway
New York 13, New York (1)

Commanding Officer
Office of Naval Research
Branch Office
1000 Geary Street
San Francisco, California (1)

Commanding Officer
Office of Naval Research
Branch Office
1030 Green Street
Pasadena, California (1)

Officer in Charge
Office of Naval Research
Branch Office, London
Navy No. 100
FPO, New York, N.Y. (5)

Library of Congress
Washington 25, D. C. (2)
Attn: Navy Research Section

Commanding Officer
Office of Naval Research
Branch Office
844 N. Rush Street
Chicago 11, Illinois (1)

II: Department of Defense and other interested Gov't. Activities

a) General

Research & Development Board
Department of Defense
Pentagon Building
Washington 25, D. C.
Attn: Library (Code 3D-1075) (1)

Armed Forces Special Weapons Project
P.O. Box 2610
Washington, D. C.
Attn: LtCol. G.F. Blunda (2)

Joint Task Force 3
12St. & Const. Ave., N.W.
(Temp. U)
Washington 25, D.C.
Attn: Major B.D. Jones (1)

b) Army

Chief of Staff
Department of the Army
Research & Development Div.
Washington 25, D. C.
Attn: Chief of Res. & Dev. (1)

Office of the Chief of Engineers
Assistant Chief for Works
Department of the Army
Bldg. T-7, Gravelly Point
Washington 25, D.C.
Attn: Structural Branch
(R.L. Bloor) (1)

Engineering Research and
Development Laboratory
Fort Belvoir, Virginia
Attn: Structures Branch (1)

Army (cont.)

Office of the Chief of Engineers
Asst. Chief for Military
Construction
Department of the Army
Bldg. T-3, Gravelly Point
Washington 25, D. C.
Attn: Structures Branch
(M. F. Carey) (1)
Protective Construction
Branch (I. O. Thornley) (1)

Office of the Chief of Engineers
Asst. Chief for Military
Operations
Department of the Army
Bldg. T-7, Gravelly Point
Washington 25, D. C.
Attn: Structures Development
Branch (W.F. Woollard) (1)

U.S. Army Waterways Experiment
Station
P. O. Box 631
Halls Ferry Road
Vicksburg, Mississippi
Attn: Col. H. J. Skidmore (1)

The Commanding General
Sandia Base, P. O. Box 5100
Albuquerque, New Mexico
Attn: Col. Canterbury (1)

Operations Research Officer
Department of the Army
Ft. Lesley J. McNair
Washington 25, D. C.
Attn. Howard Brackney (1)

Office of Chief of Ordnance
Office of Ordnance Research
Department of the Army
The Pentagon Annex #2
Washington 25, D. C.
Attn: ORDTB-PS (1)

Ballistics Research Laboratory
Aberdeen Proving Ground
Aberdeen, Maryland
Attn: Dr. C. W. Lampson (1)

c) Navy

Chief of Naval Operations
Department of the Navy
Washington 25, D. C.
Attn: OP-31 (1)
OP-363 (1)

Chief, Bureau of Ships
Department of the Navy
Washington 25, D. C.
Attn: Director of Research (2)
Code 423 (1)
Code 442 (1)
Code 421 (1)

Director, David Taylor Model Basin
Department of the Navy
Washington 7, D. C.
Attn: Code 720, Structures
Division (1)
Code 740, Hi-Speed
Dynamics Div. (1)

Commanding Officer
Underwater Explosions Research Div.
Code 290
Norfolk Naval Shipyard
Portsmouth, Virginia (1)

Commander
Portsmouth Naval Shipyard
Portsmouth, N. H.
Attn: Design Division (1)

Director, Materials Laboratory
New York Naval Shipyard
Brooklyn 1, New York (1)

Chief, Bureau of Ordnance
Department of the Navy
Washington 25, D. C.
Attn: Ad-3, Technical Library (1)
Rec, P. H. Girouard (1)

Naval Ordnance Laboratory
White Oak, Maryland
RFD 1, Silver Spring, Maryland
Attn: Mechanics Division (1)
Explosive Division (1)
Mech. Evaluation Div. (1)

Commander
U.S. Naval Ordnance Test Station
Inyokern, California
Post Office - China Lake, Calif.
Attn: Scientific Officer (1)

Naval Ordnance Test Station
Underwater Ordnance Division
Pasadena, California
Attn: Structures Division (1)

Navy (cont.)

Chief, Bureau of Aeronautics
Department of the Navy
Washington 25, D.C.
Attn: TD-41, Technical Library (1)

Chief, Bureau of Ships
Department of the Navy
Washington 25, D. C.
Attn: Code P-314 (1)
Code C-313 (1)

Officer in Charge
Naval Civil Engr. Research &
Evaluation Laboratory
Naval Station
Port Hueneme, California (1)

Superintendent
U.S. Naval Post Graduate School
Annapolis, Maryland (1)

d) Air Forces

Commanding General
U.S. Air Force
The Pentagon
Washington 25, D. C.
Attn: Res.& Development Div.(1)

Deputy Chief of Staff, Operations
Air Targets Division
Headquarters, U.S. Air Force
Washington 25, D. C.
Attn: AFOIN-T/PV (1)

Office of Air Research
Wright-Patterson Air Force Base
Dayton, Ohio
Attn: Chief, Applied Mechanics Group (1)

e) Other Government Agencies

U.S. Atomic Energy Commission
Division of Research
Washington, D. C. (1)

Director, National Bureau of Standards
Washington 25, D. C.
Attn: Dr. W.H. Ramberg (1)

Supplementary Distribution List

Addressee	No. of Copies Unclassified Reports	No. of Copies Classified Reports
Professor Lynn Beedle Fritz Engineering Laboratory Lehigh University Bethlehem, Pennsylvania	1	-
Professor R.L. Bisplinghoff Dept. of Aeronautical Engineering Massachusetts Institute of Technology Cambridge 39, Massachusetts	1	1
Professor Hans Bleich Dept. of Civil Engineering Columbia University Broadway at 117th St. New York 27, New York	1	1

Addressee	Unclassified Reports	Classified Reports
Professor B.A. Boley Dept. of Aeronautical Engineering Ohio State University Columbus, Ohio	1	-
Professor G.F. Carrier 309 Pierce Hall Harvard University Cambridge, Massachusetts	1	1
Professor R.J. Dolan Dept. of Theoretical & Applied Mechanics University of Illinois Urbana, Illinois	1	-
Professor Lloyd Donnell Department of Mechanics Illinois Institute of Technology Technology Center Chicago 16, Illinois	1	-
Professor A.C. Eringen Illinois Institute of Technology Department of Mechanics Technology Center Chicago 16, Illinois	1	-
Professor B. Fried Dept. of Mechanical Engineering Washington State College Pullman, Washington	1	-
Mr. Martin Goland Midwest Research Institute 4049 Pennsylvania Avenue Kansas City 2, Missouri	1	-
Dr. J.N. Goodier School of Engineering Stanford University Stanford, California	1	-
Professor R.M. Hermes College of Engineering University of Santa Clara Santa Clara, California	1	1
Professor R.J. Hansen Dept. of Civil & Sanitary Engineering Massachusetts Institute of Technology Cambridge 39, Massachusetts	1	1

Addressee	Unclassified Reports	Classified Reports
Professor M. Hetenyi Walter P. Murphy Professor Northwestern University Evanston, Illinois	1	-
Dr. N.J. Hoff, Head Department of Aeronautical Engineering & Applied Mechanics Polytechnic Institute of Brooklyn Brooklyn 2, New York	1	1
Dr. J.H. Hollomon General Electric Research Laboratories 1 River Road Schenectady, New York	1	-
Dr. W.H. Hoppmann Department of Applied Mechanics Johns Hopkins University Baltimore, Maryland	1	1
Professor L.S. Jacobsen Department of Mechanical Engineering Stanford University Stanford, California	1	1
Professor J. Kempner Department of Aeronautical Engineering and Applied Mechanics Polytechnic Institute of Brooklyn 99 Livingston Street Brooklyn 2, New York	1	1
Professor George Lee Department of Aeronautical Engineering Renssalaer Polytechnic Institute Troy, New York	1	-
Professor Paul Lieber Department of Aeronautical Engineering Renssalaer Polytechnic Institute Troy, New York	1	1
Professor Glen Murphy, Head Department of Theoretical & Applied Mechanics Iowa State College Ames, Iowa	1	-
Professor N.M. Newmark Department of Civil Engineering University of Illinois Urbana, Illinois	1	1

Addressee	Unclassified Reports	Classified Reports
Professor Jesse Ormondroyd University of Michigan Ann Arbor, Michigan	1	-
Dr. W. Osgood Armour Research Institute Technology Center Chicago, Illinois	1	-
Dr. R.P. Petersen, Director Applied Physics Division Sandia Laboratory Albuquerque, New Mexico	1	1
Dr. A. Phillips School of Engineering Stanford University Stanford, California	1	-
Dr. W. Prager Graduate Division of Applied Mathematics Brown University Providence 12, R. I.	1	1
Dr. S. Raynor Armour Research Foundation Illinois Institute of Technology Chicago, Illinois	1	-
Professor E. Reissner Department of Mathematics Massachusetts Institute of Technology Cambridge 39, Massachusetts	1	-
Professor M.A. Sadowsky Illinois Institute of Technology Technology Center Chicago 16, Illinois	1	-
Professor V.L. Salerno Department of Aeronautical Engineering Renssalaer Polytechnic Institute Troy, New York	1	1
Professor M.G. Salvadori Department of Civil Engineering Columbia University Broadway at 117th Street New York 27, New York	1	-
Professor J.E. Stallmeyer Talbot Laboratory Department of Civil Engineering University of Illinois Urbana, Illinois	1	1

Distribution List

Addressee	Unclassified Reports	Classified Reports
Professor E. Sternberg Illinois Institute of Technology Technology Center Chicago 16, Illinois	1	-
Professor R. G. Sturm Purdue University Lafayette, Indiana	1	-
Professor F. K. Teichmann Department of Aeronautical Engineering New York University University Heights, Bronx New York, N. Y.	1	-
Professor C. T. Wang Department of Aeronautical Engineering New York University University Heights, Bronx New York, N. Y.	1	-
Project File	2	2
Project Staff	5	-
For possible future distribution by the University	10	-
To ONR Code 438, for possible future distribution	-	10